remote sensing

MDPI

Article

Estimating Relations of Vegetation, Climate Change, and Human Activity: A Case Study in the 400 mm Annual Precipitation Fluctuation Zone, China

Yang Li [1,2,3], Zhixiang Xie [1,2,3], Yaochen Qin [1,2,3,*] and Zhicheng Zheng [1,2,3]

1 College of Environment and Planning, Henan University, Kaifeng 475004, China; liyang.rs@henu.edu.cn (Y.L.); xiezhixiang@henu.edu.cn (Z.X.); zhengzhicheng@henu.edu.cn (Z.Z.)
2 Key Laboratory of Geospatial Technology for Middle and Lower Yellow River Region, Kaifeng 475004, China
3 Collaborative Innovation Center of Urban-Rural Coordinated Development, Zhengzhou 450046, China
* Correspondence: qinyc@henu.edu.cn

Received: 11 April 2019; Accepted: 14 May 2019; Published: 15 May 2019

Abstract: The 400 mm annual precipitation fluctuation zone (75°55′–127°6′E and 26°55′–53°6′N) is located in central and western China, which is a transition area from traditional agricultural to animal husbandry. It is extremely sensitive to climatic changes. The corresponding changes of the ecosystem, represented by vegetation, under the dual influences of climate change and human activities are important issues in the study of the regional ecological environment. Based on the Savitzky–Golay (S–G) filtering method, the Global Inventory Modeling and Mapping Studies (GIMMS) Normalized Differential Vegetation Index (NDVI) dataset (NDVI3g) was reconstructed in this paper. Sen's slope estimation, Mann–Kendall (M–K), multiple regression residual analysis, and the Hurst index were used to quantify the impacts of climate change and human activities on vegetation; in addition, the future persistence characteristics of the vegetation changes trend were analyzed. Vegetation changes in the study area had an obvious spatio-temporal heterogeneity. On an annual scale, the vegetation increased considerably, with a growth rate of 0.50%/10a. The multi-year mean value of NDVI and growth rate of cultivated land were the highest, followed by the forest land and grassland. On a seasonal scale, the vegetation cover increased most significantly in autumn, followed by spring and summer. In the southeastern and central parts of the study area, the vegetation cover increased significantly ($P < 0.05$), while it decreased significantly in the northeastern and southwestern parts. In summer, the NDVI value of all vegetation types (cultivated land, forest land and grassland) reached the maximum. The change rate of NDVI value for cultivated land reached the highest in autumn (1.57%/10a), forest land reached the highest in spring (1.15%/10a), and grassland reached the highest in autumn (0.49%/10a). The NDVI of cultivated land increased in all seasons, while forest land (−0.31%/10a) and grassland (−0.009%/10a) decreased in winter. Partial correlation analysis between vegetation and precipitation, temperature found that the areas with positive correlation accounted for 66.29% and 55.05% of the total area, respectively. Under the influence of climate change alone, 62.79% of the study area showed an increasing tendency, among which 46.79% showed a significant upward trend ($P < 0.05$). The NDVI decreased in 37.21% of the regions and decreased significantly in 14.88% of the regions ($P < 0.05$). Under the influence of human activities alone, the vegetation in the study area showed an upward trend in 59.61%, with a significant increase in 41.35% ($P < 0.05$), a downward trend in 40.39%, and a significant downward trend in 7.95% ($P < 0.05$). Vegetation growth is highly unstable and prone to drastic changes, depending on the environmental conditions.

Keywords: vegetation; climate change; human activity; GIMMS NDVI3g; 400-mm annual precipitation fluctuation zone

1. Introduction

The fifth assessment report of the Intergovernmental Panel on Climate Change (IPCC) points out that almost all regions of the world are experiencing climate warming, and since 1950, precipitation in Asia has been significantly decreasing [1]. Climate change will inevitably affect the growth environment of plants, and thus, the growth state of plants. Vegetation changes, along with the changes in regional hydrothermal conditions, such as solar radiation, atmosphere, water, and soil energy transmission, show interannual and seasonal variation characteristics and are indicators of global climatic changes [2,3]. With the rapid development of remote-sensing technology in recent years, remote-sensing data has become the main data source for the study of vegetation changes in long time series with high spatial and temporal resolution [4,5]. For example, the Normalized Differential Vegetation Index (NDVI) has a good correlation with the biomass and leaf area index and can, therefore, adequately reflect the growth status of surface vegetation [6]. Against the background of climatic changes and enhanced human activities, terrestrial ecosystems have undergone significant changes [7], and vegetation changes have recorded the imprint of human activities profoundly [8]. In this sense, vegetation has become the focus and core issue of scholars in the context of climate change due to its strong indicative effect on the ecological environment [9–11].

The transition zone is the intersection zone between adjacent ecosystems and represents a key location for terrestrial ecosystems to respond to climate change and human activities. The transition zone between agriculture and animal husbandry, which takes the 400 mm annual precipitation line as the dividing line, is a transitional land-use mode and a transition zone between grassland and cultivated land, the planting industry, and animal husbandry [12]. Most of the world's semi-arid regions are farming-pastoral zones, and the four major agricultural and pastoral ecotones in the world are the northeast and southwest agricultural and pastoral ecotone in China, the east–west agricultural and pastoral ecotone in the southern margin of the Sahara desert in Africa, the southwest agricultural and pastoral ecotone in the west of the United States, and the agricultural and pastoral ecotone at the junction of Russia and Kazakhstan [13]. Under a changing climate, the natural elements of the transition zone are extremely sensitive, and the stability of the original appearance of the natural environment is relatively low. The system evolves easily, and once such evolution occurs, it is irreversible, and the ecological environment is sensitive and fragile. Therefore, it is important to quantify the contribution of the climate and of human activities to the evolution of vegetation.

The 400 mm annual precipitation fluctuation zone covers most of China's arid and semi-arid regions. In recent years, research on the response of vegetation to climate change and human activities in the transition zone of agriculture and animal husbandry in China has attracted considerable attention. In terms of regional selection, studies have been carried out in regions where the coupling effect between vegetation and climate change and human activities is typical within the fluctuation area of the 400 mm annual precipitation line, for example on the Loess Plateau [14–16], in the northeast of China [17,18], on the Qinghai–Tibet Plateau [19–21]. Shi et al. [22] have found that climate change and human activities had a significant driving effect on the boundary change of the northern farming-pastoral ecotone, and some studies quantitatively analyzed the impacts of climate change and human activities on arable land [23,24]. Sun et al. [25] have found that vegetation coverage on the Loess Plateau showed a significant upward trend in the past three decades under the influence of human activities, mainly ecological restoration projects. Global warming is beneficial to vegetation growth in regions with strong water-bearing capacity, while vegetation growth is severely restricted in regions with poor water resources [26,27]. Studies have found that precipitation is the most important factor affecting vegetation growth on the Mongolian plateau [28], and the spring climate warming can only promote the early greening of the meadow steppe vegetation, while the water shortage of the typical steppe vegetation and desert steppe vegetation may eliminate the impacts of climate warming [29]. At present, unitary linear regression is mostly used to analyze interannual changes in vegetation in research on vegetation change trends, but this method has a weak ability to avoid errors [30]. Vegetation NDVI changes are the result of joint action between climate change and human activity [31,32], but previous

studies have paid more attention to the response of vegetation NDVI to climate change from the perspectives of natural elements. As the influence of human activities on vegetation can mainly be described qualitatively, how to quantify the impacts of human activities is one of the important topics that needs to be investigated in more detail [33]. In addition, in terms of the selection of adequate research regions, previous studies have focused mainly on several subregions of extremely typical regions within the transition zone of agriculture and animal husbandry, but have mostly failed to study the spatial range of the fluctuation regions of 400 mm annual precipitation lines.

On the basis of quantifying climate and vegetation change, this study focuses on assessing the impact of climate change and human activities on vegetation change. The interaction mechanism between climate change, human activities and vegetation growth was discussed in depth in this study to provide a theoretical basis and scientific support for the coupling research of the human–Earth system.

2. Materials and Methods

2.1. Study Area

The designation of the study area was based on the historical period of the meteorological station precipitation data. The annual precipitation fluctuation zone [34] covers 17 provinces and autonomous regions, including Heilongjiang, Jilin, Liaoning, Hebei, Inner Mongolia, Shanxi, Shaanxi, Gansu, Ningxia, Sichuan, Qinghai, Xinjiang, Tibet, Shandong, Henan, Beijing, and Tianjin, with an area of about 3.56 million km^2 (Figure 1). The regions with large precipitation are mainly distributed in the south of the study area; the average annual precipitation in the entire study area was about 500 mm from 1951–2015. The study area spans the first, second, and third steps of China, with a large elevation drop and an extremely complex terrain. The study area is close to the pastoral area in the northwest, with a higher proportion of grassland, and close to the agricultural area in the southeast, with a higher proportion of arable land.

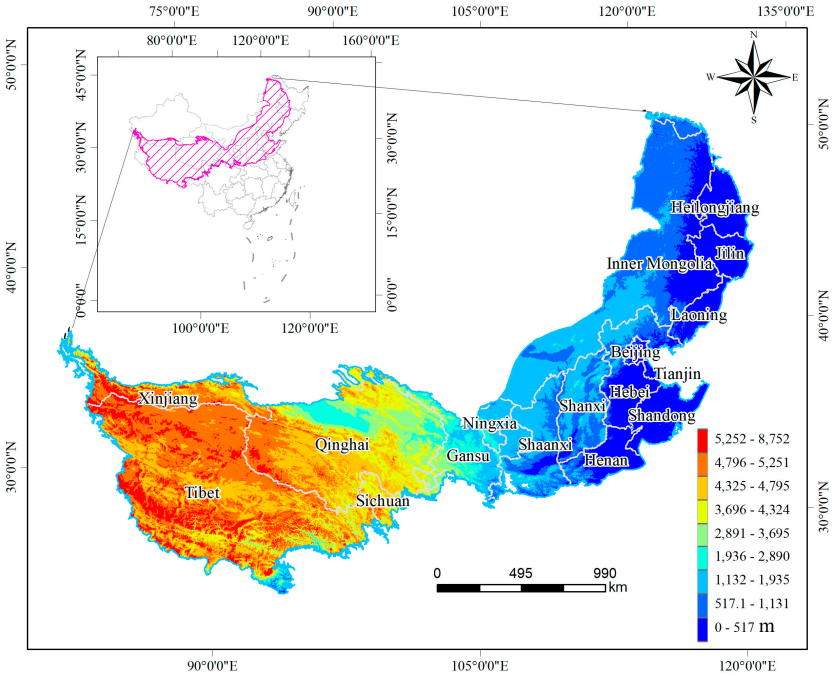

Figure 1. The geographical location of the 400 mm annual precipitation fluctuation zone and digital elevation model.

2.2. Global Inventory Modeling and Mapping Studies Normalized Differential Vegetation Index (GIMMS NDVI3g) Dataset

The AVHRR Global Inventory Modelling and Mapping Studies (GIMMS) NDVI3g remote-sensing datasets are the latest version of the global vegetation dataset from 1982 to 2015, launched by the National Aeronautics and Space Administration (NASA) Ames Ecological Forecasting Lab (http://ecocast.arc.nasa.gov). The GIMMS NDVI3g dataset with the temporal resolution of monthly and the spatial resolution of 8 × 8 km. Because GIMMS NDVI3g data has large signal noise, the premise of relevant research is to reconstruct the NDVI time-series data of vegetation. Considering the advantages of S–G filtering in the reconstruction of NDVI vegetation data, for example, the data set of the NDVI sequence reconstructed by the S–G filtering algorithm can effectively remove the influence of outliers, better retain the continuity characteristics of vegetation growth changes, and does not change the numerical value of the continuity changes. Therefore, this paper adopts the S–G filtering method to reconstruct NDVI timing sequence data.

2.3. Climate Dataset

The temperature and precipitation data of the 2474 meteorological stations were obtained from the China meteorological data-sharing network (http://data.cma.cn/). The original time resolution of the meteorological dataset was daily, which was converted into monthly and yearly in this study. All data were obtained through field observation. It provides complete statistical analysis, data diagnosis, and spatial distribution standard error. The ANUSPLIN software is a tool for interpolating multivariable data using thin disk smooth spline interpolation, and this study used ANUSPLIN (Australian National University, Canberra, Australia) to perform interpolation analysis on the precipitation data of 2474 meteorological stations across the Chinese mainland from 1951 to 2015 and the temperature data from 1982 to 2015, thereby obtaining grid data (8 × 8 km) of the temperature and precipitation in each year within the Chinese mainland during the corresponding period.

2.4. Methods

2.4.1. Sen's Tendency Estimation

The Sen slope estimation method is suitable for the qualitative description of time series with obvious trends. Although it is also a mathematical statistical method, it is in essence a qualitative method for describing the trend of sequences. At the same time, the advantage of Sen's slope estimation method is that even the lack of data or the existence of bad points in individual data series do not affect the trend result. In this paper, the tendency of NDVI time series was calculated by Sen's estimation method. For the time series $x_t = (x_1, x_2, \ldots, x_n)$, is the formula was as follows:

$$\beta = Median\left(\frac{x_j - x_i}{j - i}\right), \forall_{j>i} \quad (1)$$

where β is the tendency of the NDVI sequence, x_i, x_j are the sequences of NDVI, i, j is the year of the NDVI. When the calculated result of β is greater than 0, the time series shows an upward trend; when the calculated result of β is less than 0, the time series shows a downward trend.

2.4.2. Mann–Kendall (M–K) Significance Test

In this paper, the significance of the linear variation trend of the NDVI was tested by the M–K trend test. Since this method does not require sample data to obey a certain distribution and is less

affected by outliers, it can be used to effectively test the variation trend of the NDVI in time series. The formulas are as follows:

$$Z = \begin{cases} \frac{S-1}{\sqrt{s(S)}} & S > 0 \\ 0 & S = 0 \\ \frac{S+1}{\sqrt{s(S)}} & S < 0 \end{cases} \quad (2)$$

$$S = \sum_{j=1}^{n-1} \sum_{i=j=1}^{n} sgn\left(NDVI_j - NDVI_i\right) \quad (3)$$

$$sgn\left(NDVI_j - NDVI_i\right) = \begin{cases} 1 & NDVI_j - NDVI_i > 0 \\ 0 & NDVI_j - NDVI_i = 0 \\ -1 & NDVI_j - NDVI_i < 0 \end{cases} \quad (4)$$

$$s = \frac{n(n-1)(2n+5)}{18} \quad (5)$$

where $NDVI_i$ and $NDVI_j$ are the NDVI values of the pixels in the ith and jth years, n represents the length of time series, sgn is a symbolic function, and the Z value is $(-\infty, +\infty)$. Under the given significance level ($P < 0.05$), there is a significant change when $|Z| >$ u1-α/2. When $|Z| > 1.96$, it means that the linear trend has passed the significance test of 0.05. When $|Z| > 2.58$, it has passed the significance test of 0.01.

2.4.3. Multiple Regression and Residual Analysis

Due to the lack of long time series observation data of the impact of human activities on vegetation NDVI, it is difficult to directly quantify the impact of human activities on vegetation. In this paper, the effects of climate change and human activities on vegetation were quantified by multiple regression analysis and residual analysis. The theoretical basis of this method is that under natural conditions NDVI is only affected by climate change, so it can be understood that in the absence of human influence, the change characteristics of NDVI should be consistent with those of climate change [35]. The multiple regression residual method [36,37] was used to quantify the impacts of climate factors on vegetation. Temperature and precipitation, two climate factors that mainly affect vegetation [38,39], were used as independent variables, and vegetation values were used as dependent variables for regression. Through regression analysis, the equation characterizing the correlation between vegetation NDVI, temperature and precipitation was obtained. Then, the annual temperature and precipitation data from 1982 to 2015 were respectively put into the equation to obtain the vegetation $NDVI_{pre}$. The predicted value of $NDVI_{pre}$ was taken as the impact of climate factors on vegetation NDVI without interference of human activities. Finally, the residual analysis was adopted to quantify the contribution of human activities on vegetation by calculating the difference between the remote-sensing data and the predicted value [40,41]. The formulas are as follows:

$$NDVI_{pre} = A \times T + B \times P + C \quad (6)$$

where $NDVI_{pre}$ is the NDVI simulation value, T is the average temperature, P is precipitation, A, B are regression coefficients, and C is a constant.

This paper defines the impact of human activities on vegetation as all impacts except the impact of climate change on vegetation. The calculation formula is as follows:

$$NDVI_{res} = NDVI_{obs} - NDVI_{pre} \quad (7)$$

where $NDVI_{res}$ is the residual error, that is, the NDVI value under the influence of human activities alone, $NDVI_{obs}$ is the remote-sensing data value, $NDVI_{pre}$ is the vegetation NDVI value under the influence of climate change alone. In this study, $NDVI_{res}$ and $NDVI_{pre}$ from 1982 to 2015 were analyzed

to obtain the NDVI change trend under the influence of human activities and climate change. If the trend is positive, it indicates that human activities or climate change have a promoting effect on vegetation growth. A negative trend indicates an inhibitory effect on vegetation growth.

2.4.4. Hurst Index

The Hurst index method [42], which is based on the R/S analysis method, is generally used to analyze the fractal characteristics and long-term memory process of time series. It is an effective method to quantitatively describe the long-term dependence of time series information and is now widely used to judge the intensity of persistence or anti-persistence of the change trend of time series [43,44]. The Hurst index method was used to study the spatial distribution and persistence of vegetation change trend in the 400 mm annual precipitation line fluctuation area. The calculation steps are as follows, for the time series of $NDVI_t$, t = 1, 2, 3, 4, 5, . . . , n:

$$\overline{NDVI}_{(\tau)} = \frac{1}{\tau}\sum_{t=1}^{\tau} NDVI_{(\tau)} \quad \tau = 1, 2, 3, \ldots, n \tag{8}$$

$$X_{(t,\,\tau)} = \sum_{j=1}^{t}\left(\mathrm{NDVI}_{(j)} - \overline{\mathrm{NDVI}}_{(\tau)}\right) \quad 1 \le \ t \le \tau \tag{9}$$

$$R_{(\tau)} = \underset{1\le t\le\tau}{max} X_{(t,\tau)} - \underset{1\le t\le\tau}{min} X_{(t,\tau)} \quad \tau = 1, 2, 3, \ldots, n \tag{10}$$

$$S_{(\tau)} = \left[\frac{1}{\tau}\sum_{t=1}^{\tau}\left(NDVI_{(t)} - NDVI_{\tau}\right)^2\right]^{\frac{1}{2}} \quad \tau = 1, 2, 3, \ldots, n \tag{11}$$

$$\frac{R(\tau)}{S(\tau)} = (c\tau)^H \tag{12}$$

The value of H ranges from 0 to 1. When $0.5 < H < 1$, the future change of the NDVI will be consistent with the changing trend in the past; when $H = 0.5$, the changes before and after the time series of the NDVI are independent, and when $0 < H < 0.5$, the NDVI will show trend opposite to that from the past.

2.4.5. Partial Correlation Analysis

Temperature and precipitation are the variables most closely related to vegetation growth. In this study, partial correlation analysis method was adopted to study the correlation between vegetation NDVI and temperature by using precipitation as the control variable. Secondly, temperature was used as the control variable to analyze the partial correlation between vegetation NDVI and precipitation. Partial correlation analysis is carried out on the basis of correlation calculation, and the specific calculation formula is as follows:

$$R_{xy} = \frac{\sum_{i=1}^{n}(x_i - \overline{x})(y_i - \overline{y})}{\sqrt{\sum_{i=1}^{n}(x_i - \overline{x})^2}\sqrt{\sum_{i=1}^{n}(y_i - \overline{y})^2}} \tag{13}$$

where: R_{xy} is the correlation coefficient; x_i and y_i represent the values of variables x and y at period i, respectively. x and y represent the average of the variables x and y; n is the sample size. The value range of the correlation coefficient is −1 ~ 1.

$$R_{xy,z} = \frac{R_{xy} - R_{xz}R_{yz}}{\sqrt{\left(1 - R_{xz}^2\right)\left(1 - R_{yz}^2\right)}} \tag{14}$$

where: $R_{xy,z}$ is the partial correlation coefficient between variables x and y when the variable z is regarded as a constant; R_{xy}, R_{xz}, R_{yz} represent the correlation coefficients between x, y and z, respectively. The partial correlation coefficient ranges from −1 to 1.

3. Results

3.1. Spatial and Temporal Patterns and Variations Analysis

3.1.1. Temperature and Precipitation

Figure 2 shows the spatial pattern of average annual precipitation, temperature and its interannual change trend from 1951 to 2015. The average annual precipitation and temperature show an obvious spatial heterogeneity. The average annual precipitation in the eastern and southern parts (> 800 mm) of the study area is significantly higher than that in the northwest (< 300mm), and the precipitation in Inner Mongolia, Ningxia and the central and western parts of Qinghai is extremely scarce (Figure 2a). The average annual temperature is higher in the middle (> 12 °C) and lower at both ends of the study area. The average annual temperature in the southeast of the study area (Shaanxi, Shanxi, Henan, Hebei and Shandong) was highest (11.23 °C), followed by Inner Mongolia, Liaoning, Jilin and Heilongjiang. The Qinghai–Tibet Plateau region has the lowest average annual temperature (−1.44 °C) due to high elevation (Figure 2b). According to the change trend of precipitation from 1951 to 2015 (Figure 2c), except Qinghai and Heilongjiang, the annual precipitation showed a decreasing trend in most regions. The annual precipitation in the vast western region of Tibet showed a significant downward trend (<−6 mm/a). The increase of temperature is most obvious in the Qinghai–Tibet Plateau, followed by the Loess Plateau and the northwest edge of Inner Mongolia (Figure 2d). The temperature increased slightly in Henan, Hebei, Shandong, Liaoning, Jilin and Heilongjiang in the southeast of the study area. In general, the study area generally shows a warming trend, in which the northwest and the Qinghai–Tibet Plateau region have a higher warming tendency.

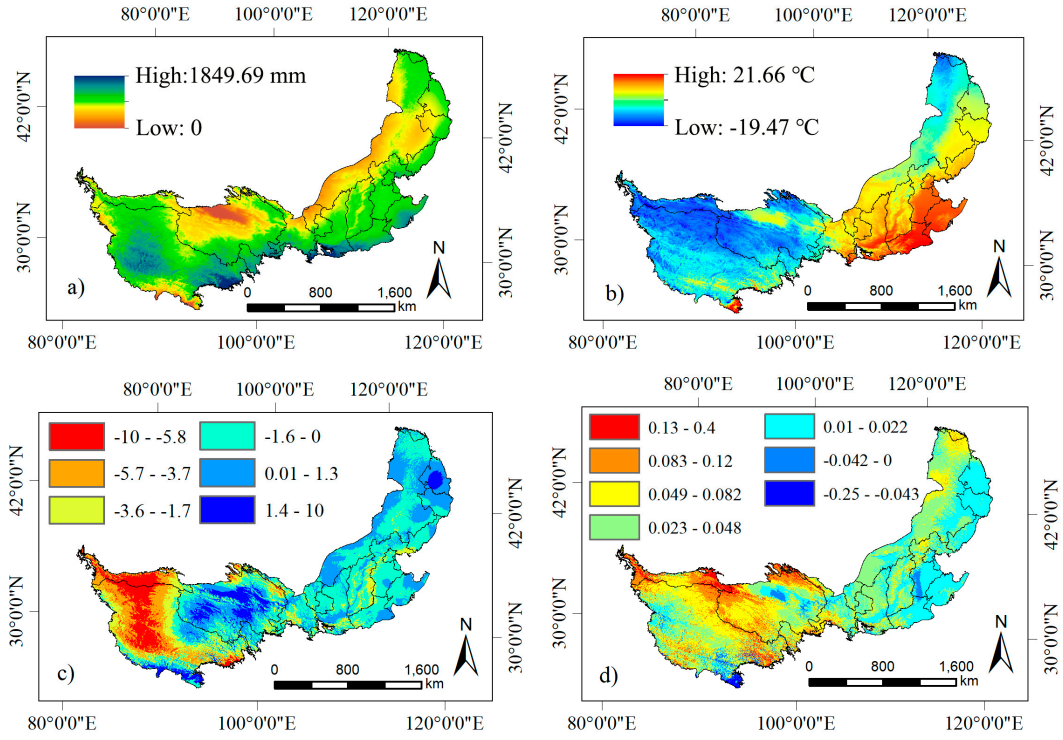

Figure 2. The spatial pattern and variation trend of average annual precipitation and temperature from 1951 to 2015 (**a**): Precipitation, (**b**): Temperature, (**c**): Precipitation variation trend; (**d**): Temperature variation trend.

3.1.2. Vegetation Patterns and Variations on Annual Scales

From 1982 to 2015, the spatial distribution of the average annual vegetation NDVI with temporal resolution yearly in the study area showed obvious spatial heterogeneity (Figure 3a). Generally speaking, it shows the distribution rule of vegetation NDVI is higher in the southeast, lower in the northwest and decreasing from southeast to northwest. The average annual change rate of the NDVI was 0.45%/10a, indicating that the overall vegetation in the study area presented a gradually increasing trend. The regions with high NDVI values are mainly distributed in the Greater Hinggan mountains in the northeast of Inner Mongolia, Henan, southern Shaanxi, Gansu, Qinghai, and southeast Tibet. In contrast, the regions with low NDVI values are mainly distributed in Ningxia, Gansu, on the Inner Mongolia plateau, in Qinghai, and in northwest Tibet. Among them, the low NDVI values in Qinghai and the northwest of Tibet are caused by the perennial low temperature in the region as a result of the elevation, while the low precipitation and water resource shortage in Ningxia, Gansu, and parts of the Inner Mongolia plateau, which are deeply inland, further increase the evaporation capacity due to climate warming and aggravate regional droughts. To study the characteristics of vegetation NDVI changes over time, based on the NDVI data set from 1982 to 2015, this paper adopts the Sen trend analysis method to analyze the change trend pixel by pixel (Figure 3b). Based on the results, the change trend of vegetation in the study area decreases at both ends and increases in the middle part of the space. Increases in the NDVI are mainly distributed in Shanxi, Shaanxi, and the border areas of Shandong, Henan, and Hebei. The values of the NDVI decreased in northeast Inner Mongolia (−2.3%/10a) and on the central Qinghai–Tibet Plateau (−1.4%/10a). The M-K method was used to test the significance of the NDVI variation trend, and the spatial distribution of regions with significant variation ($p < 0.05$) and extremely significant variation ($p < 0.01$) was roughly consistent (Figure 3c,d). The NDVI values were significantly increased, and the regions that passed the significance test were mainly distributed in the border areas of Shaanxi, Shanxi, and Henan, and Hebei and Shandong. The NDVI increased by 2.4 and 5.9%/10a; the regions where the NDVI value decreased significantly and passed the significance test were mainly distributed in the Greater Hinggan mountains of Inner Mongolia, Qinghai, and the south-central part of Tibet. Figure 3e is the land-use type diagram of the research area, and Figure 3f is the multi-year mean value of NDVI and its change slope of each land type (cultivated land, forest land and grassland). From the perspective of the NDVI value of land types, forest land has the highest NDVI value (0.41), followed by cultivated land (0.37), and grassland has the lowest NDVI value (0.24). From the perspective of the change slope of NDVI of each land type, cultivated land increased the fastest (0.79%/10a), followed by forest land (0.72%/10a) and grassland (0.2%/10a).

Referring to the research carried out in arid and semi-arid regions [45] and combining with the specific actual conditions in this study area, the NDVI values in the study area were divided into six grades. Table 1 shows the proportion of the coverage area of each grade in the total area of the study area. The vegetation coverage area (NDVI > 0.1) accounts for 90.2% of the total study area, but the overall vegetation coverage of the study area is low. The average NDVI value is only 0.29, with a minimum of 0.018, and the standard deviation is 0.14. Among the six grades, the area with NDVI values between 0.3 and 0.4 accounted for the largest proportion (24.37%), followed by the area with NDVI values between 0.2 and 0.3, accounting for 22.81%. Non-vegetated areas accounted for 9.8% of the total area and were mainly composed of lakes, Gobi, and deserts. Areas with NDVI values higher than 0.4 accounted for 21.98% of the total area, and the vegetation types under the NDVI grade were mainly woodland.

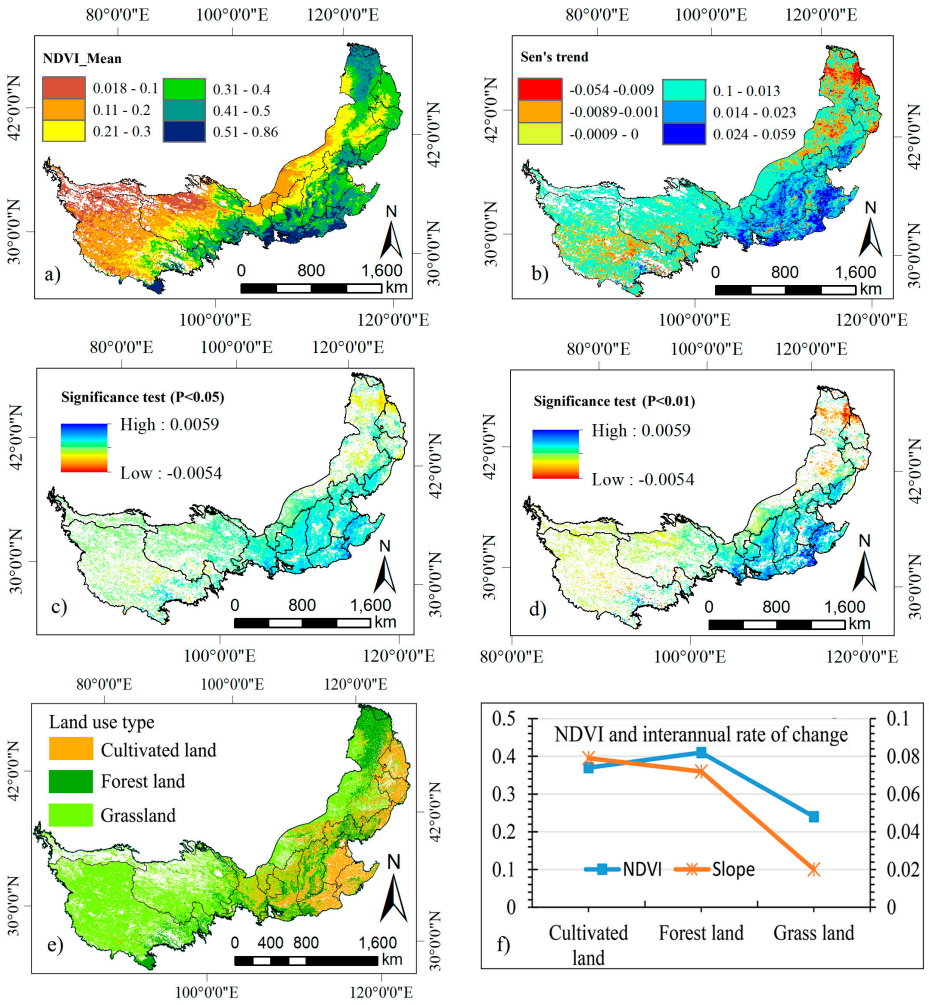

Figure 3. Vegetation spatial pattern, interannual variation trend and significance test. (**a**) NDVI_mean; (**b**) Sen's trend/10a; (**c**) Significance test ($P < 0.05$); (**d**) Significance test ($P < 0.01$); (**e**) Land use type; (**f**) Normalized Differential Vegetation Index (NDVI) and interannual rate of change.

Table 1. Area statistics of NDVI values of each grade (Unit: %).

Level	NDVI < 0.1	0.1 < NDVI<0.2	0.2 < NDVI < 0.3	0.3 < NDVI < 0.4	0.4 < NDVI < 0.5	0.5 < NDVI < 0.8
Area	9.80	21.04	22.81	24.37	16.37	5.61

3.1.3. Vegetation Patterns and Variations on Seasonal Scales

Figure 4 shows the spatial pattern and variation trends of the NDVI on a seasonal scale for the period from 1982 to 2015. From the perspective of the seasonal scale, the average NDVI trend rate of vegetation in spring was 0.72%/10a, and the areas with significantly increased values were mainly concentrated in Henan, Shandong, and southern Shaanxi on the southeastern edge of the study area. This was because the temperature increased earlier in the spring in the above areas, and the water conditions were better, resulting in an earlier start of the growing season. The regions where NDVI decreased were mainly distributed along the border of Inner Mongolia, Heilongjiang and Liaoning, and the northwest of Tibet (Figure 4a). The mean trend rate of the NDVI in summer was 0.52%/10a, and the areas of continuous increase were mainly located in northern Shaanxi, Shanxi, and Liaoning (Figure 4b). Compared with the areas of gradual NDVI decreases in spring, they were spatially shifted from the junction of three provinces to the northeast of Inner Mongolia. In addition, the vegetation in the central part of Tibet also showed a trend of continuous decline in summer. This phenomenon

may be related to the continuous decrease of precipitation in this region in recent years (Figure 3c). The mean change rate of the NDVI in autumn was 0.79%/10a (Figure 4c). The area with increasing values was basically consistent with that in summer, while the area with decreasing values moved to the central region of Inner Mongolia. The average trend rate of the NDVI in winter was 0.003%/10a, and the regions with increasing NDVI values were mainly distributed in the border areas of southern Shaanxi, Henan, Shandong, and Hebei, while the regions with decreasing NDVI values covered the entire northeast. In winter, the decrease in NDVI was most pronounced. The reason may be that under the background of global warming, the warming and drying trend of climate in the middle and high latitudes of China gradually strengthens [46]. The rise of temperature increases the evaporation of soil water and the extension of vegetation growth period, which indirectly increases the consumption of water by vegetation. As a result, the water shortage is more serious in winter when the precipitation is extremely poor, which eventually leads to the reduction of vegetation NDVI. In addition, the NDVI values in the central region of Tibet also showed an obvious downward trend in winter (Figure 4d). In this study, the four seasons were defined as: spring (March, April and May), summer (June, July and August), autumn (September, October and November), and winter (December, January and February). In terms of seasonal scale (Table 2), the vegetation NDVI of cultivated land (0.57), forest land (0.71) and grassland (0.37) was the highest in summer. Among the four seasons, the vegetation NDVI of forest land was the highest, followed by cultivated land and grassland. The NDVI change rate of cultivated land reached the highest in autumn (1.57%/10a), the NDVI change rate of forest land was the highest in spring (1.15%/10a), and the NDVI change rate of grassland was the highest in autumn (0.49%/10a). The vegetation NDVI of cultivated land increased in all seasons, while forest land (−0.31%/10a) and grassland (−0.009%/10a) decreased in winter.

Table 2. The average NDVI of each land use types and its variation on seasonal scale from 1982–2015.

Land Use Type	Average NDVI Value				Rate of Vegetation Change (%/10a)			
	Spring	Summer	Autumn	Winter	Spring	Summer	Autumn	Winter
Cultivated land	0.34	0.57	0.39	0.22	1.43	1.07	1.57	0.38
Forest land	0.40	0.71	0.48	0.29	1.15	0.24	1.14	−0.31
Grassland	0.19	0.37	0.25	0.15	0.43	0.43	0.49	−0.009

The significance test results of vegetation variation trends in each season (Figure 4e–h) showed that NDVI increased in spring and autumn, and the area that passed the significance test ($P < 0.05$) was the largest, mainly concentrated in the southern parts of Shaanxi, Shanxi, Hebei, and Inner Mongolia, while the area with significantly increasing NDVI values in winter was the smallest. The area with NDVI decreases in winter was the largest, followed by those with decreases in spring and summer. In terms of time scale, from 1982 to 2015, the increase rate of NDVI in the study area was the highest in autumn, followed by spring and summer. In terms of spatial scale, NDVI increased most significantly in the middle part of the study area, especially in Shaanxi, Shanxi, Henan, Shandong, and Hebei, and the most obvious downward trends were observed in Inner Mongolia, Qinghai, and Tibet. From the perspective of spatial and temporal dynamics of vegetation changes, vegetation NDVI changes in different seasons showed an obvious spatial heterogeneity. The region with a high growth rate of vegetation shifted with the spatial and temporal changes of hydrothermal conditions, that is, it was concentrated in the southeastern edge of the study area in spring, gradually moved from southeast to northwest in summer and autumn to northern Shaanxi and southern Inner Mongolia and retreated to the southeastern edge of the study area in winter. Similarly, the spatial evolution of regions with significantly reduced NDVI values was also accompanied by seasonal changes. such as regions with a decreasing NDVI were distributed in the southeastern edge of the northeastern region of the study area in spring. In summer, it moved to the western edge of the northeast, while in autumn, it continued to move to central Inner Mongolia. In winter, it moved back to the northeast of the study area (Figure 4a–d).

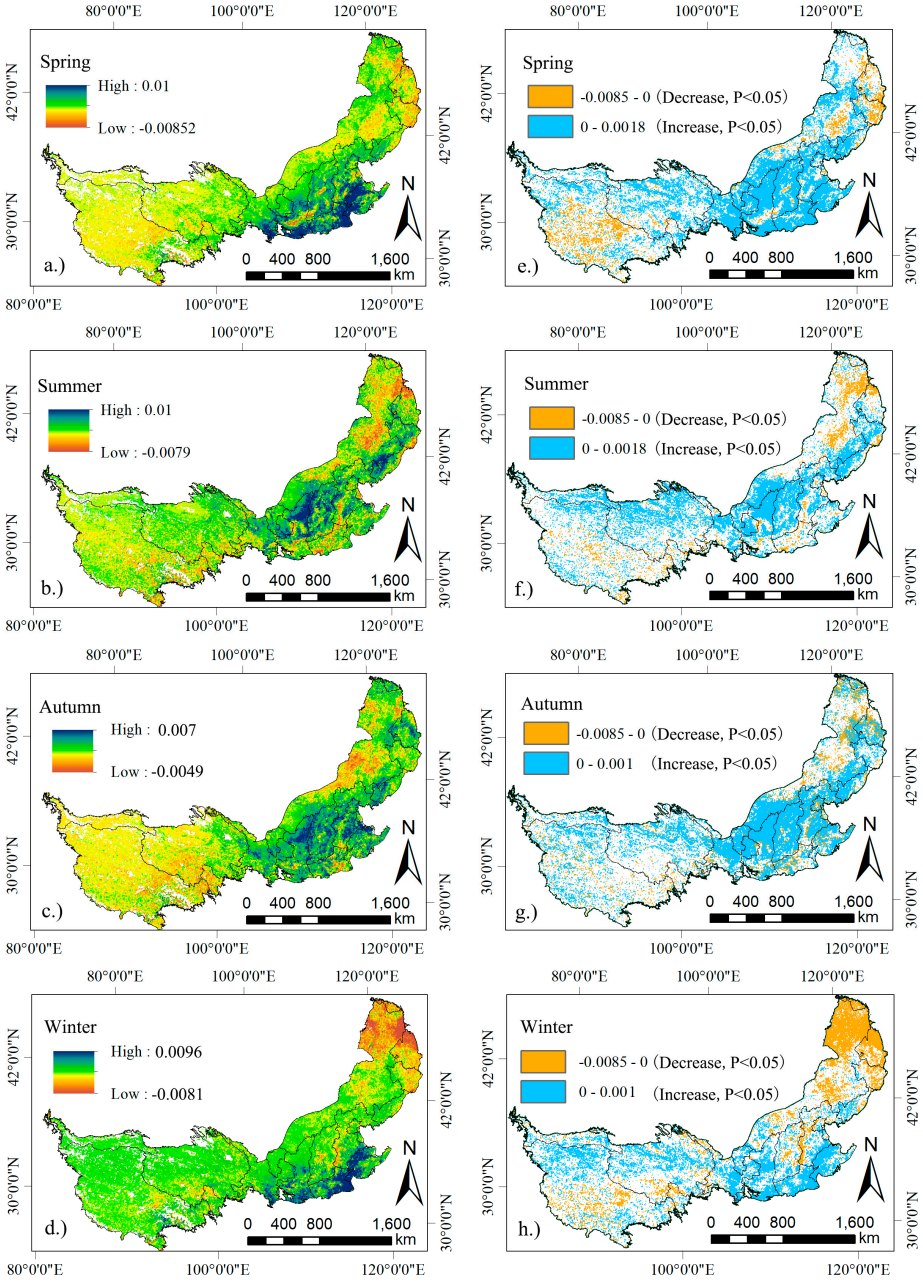

Figure 4. Vegetation NDVI variation trend and significance test of seasonal vegetation (**a**–**h**).

3.1.4. Persistence Analysis of Vegetation Variations Trend

Based on the Sen's trend and Hurst index of NDVI on annual and seasonal scales, the persistence characteristics of future vegetation change trends can be obtained (Figure 5 and Table 2). From the perspective of a seasonal scale, the regions with significant increases in NDVI in spring and a strong persistence in the future are mainly distributed in the southeastern and central regions with relatively good hydrothermal conditions. In contrast, the regions with significant decreases in NDVI and persistence in the future are mainly distributed in the central and western regions of Tibet. The NDVI increased significantly in northern Shaanxi, but the regions with anti-persistence will be concentrated in the north of Shaanxi. The regions with NDVI decreased significantly, but regions with the characteristics of anti-persistence were concentrated in the central south of Shaanxi, the southwest of Shanxi, the northeastern edge of Inner Mongolia, Heilongjiang, and the west of Jilin. At the same time, there were sporadic distributions in the southeast of the Qinghai-Tibet Plateau (Figure 5a). In summer, the NDVI

decreased significantly, but in the future, the area with anti-persistence will increase rapidly in summer compared to spring, while moving towards the west. The area of vegetation increased significantly and with persistence in the future will decrease compared with that in spring, which mainly be concentrated in Shaanxi, Shanxi, eastern Gansu, western Hebei, Liaoning, and Jilin (Figure 5b). In autumn, the NDVI decreased significantly, but in the future, the area with anti-persistence characteristics will decrease significantly compared with that in summer, with the main distributions in the central and western parts of Inner Mongolia and the southeastern edge of the Qinghai–Tibet Plateau. In autumn, the NDVI will increase significantly, and the area with strong persistence in the future will reach the maximum (1,131,597 km^2), covering the entire central and southern parts of the study area (Figure 5c). In winter, the NDVI will decrease significantly in the entire northeastern part of the study area in areas with anti-persistence characteristics, with a small range distribution on the Qinghai–Tibet Plateau. In the future, the NDVI will be significantly increased in regions with strong persistence characteristics, such as central and southern Shaanxi, central and northern Henan, and central and western Shandong (Figure 5d). On an annual scale, the regions with significantly increasing NDVI values in the future, but with strong anti-persistence characteristics, will be concentrated in northern Shaanxi, north-central Shanxi, western Liaoning, Shandong, and Hebei. In general, the NDVI will increase significantly (Figure 5e).

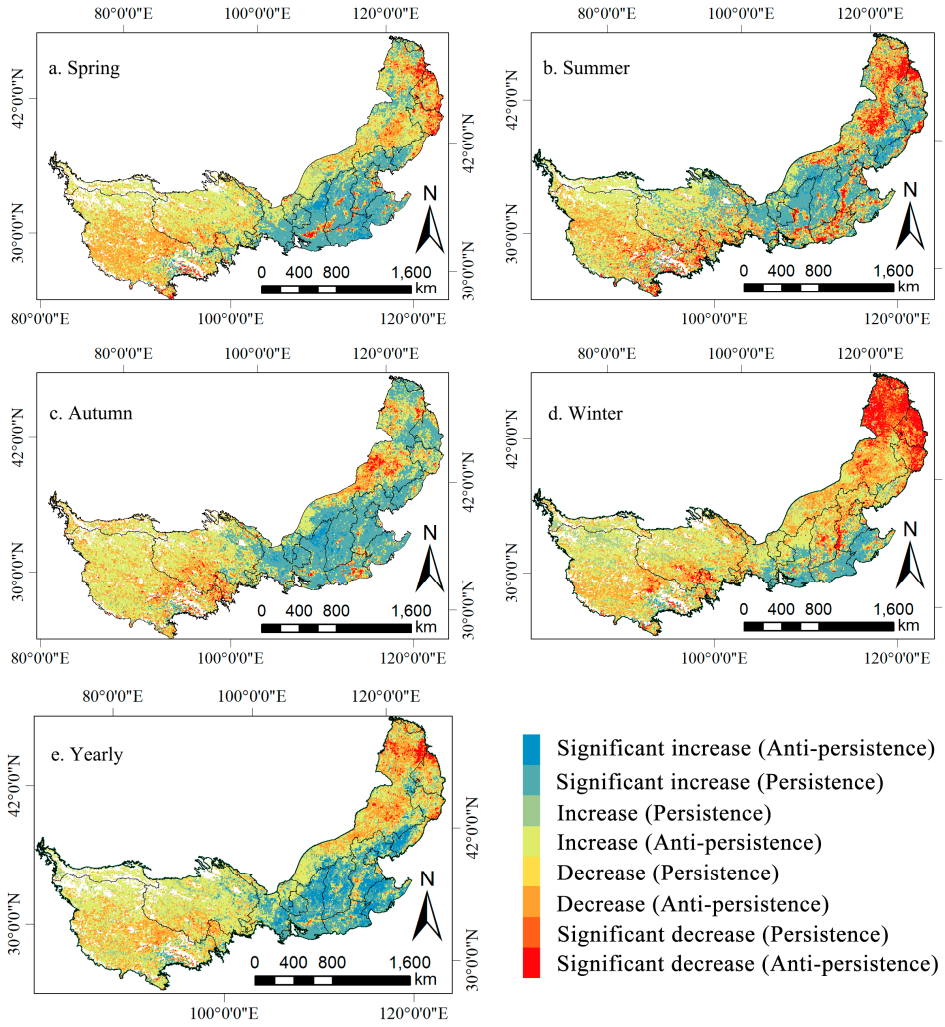

Figure 5. Persistence of the change trends of NDVI on annual and seasonal scales (**a**–**e**).

Table 3 shows the persistence statistics of annual and seasonal NDVI variation trends in the future. On each time scale, the proportion of NDVI in the region with persistence characteristics increased

significantly in autumn, reaching 32.82%. The area of vegetation with persistence and anti-persistence characteristics in the future is 28,791 km^2 and 109,187 km^2 at the annual scale, respectively. In the future, the area of NDVI with anti-persistence will be larger than that with persistence on annual scales. The regions with increasing NDVI values and an anti-persistence feature account for the largest proportion (43.60%) in the annual scale, followed by autumn (41.32%), spring (40.69%), winter (38.17%) and summer (37.08%). The area of vegetation NDVI with anti-persistent properties in the study area is greater than persistence, showed that although the area of vegetation in recent decades was restored, but due to the environmental bearing capacity being limited, especially the water resources carrying capacity, coupled with environmental fragility and instability characteristics, makes the vegetation degeneration may exist in the future.

Table 3. Persistence statistics of NDVI annual and seasonal scale variation trends in the future (unit: %).

Level	Significant Increase	Persistence Increase	Decrease	Significant Decrease	Significant Increase	Anti-Persistence Increase	Decrease	Significant Increase
Spring	24.03	3.61	2.85	0.52	2.51	40.69	22.75	3.03
Summer	25.18	2.13	1.55	0.70	3.20	37.08	22.08	8.08
Autumn	32.82	0.01	0.81	0.14	2.50	41.32	19.49	2.90
Winter	9.97	6.50	5.06	2.42	0.90	38.17	27.60	9.40
Year	14.76	8.20	4.13	0.53	7.85	43.60	18.93	2.00

3.2. Impacts of Climate Change and Human Activities on Vegetation

3.2.1. Estimating Relations of Vegetation, Temperature, and Precipitation

Figure 6a is the partial correlation analysis results between vegetation and temperature, the areas with positive correlation account for 66.29% of the total area. The areas with higher correlation coefficient were distributed in mountainous areas such as Yanshan mountain, Taihang mountain, Qinling mountain and Taishan mountain. The regions with negative correlation between vegetation and temperature were mainly concentrated in Inner Mongolia, northwest Shaanxi and north Qinghai where lack of rainfall for a long period. In addition, in plain areas with relatively low elevation, such as southern Hebei, northern Shandong and northern Henan, vegetation is negatively correlated with temperature. The correlation analysis results between vegetation and precipitation show that the precipitation is positively correlated with vegetation in 55.05% of the study area, indicating that precipitation is the main limiting factor for vegetation growth in the study area (Figure 6b). However, the spatial distribution of the correlation coefficients between vegetation and precipitation has no obvious rule, which is closely related to the randomness and suddenness of precipitation events on the space-time scale. The vegetation and precipitation show good positive correlation in northeast Inner Mongolia and west Heilongjiang (R = 0.65), southwest Henan and Qinling mountains (R = 0.34), northeast and southwest of the Qinghai–Tibet Plateau (R = 0.44), and the junction area of Shandong, Henan and Hebei (R = 0.42). Among them, the regions of northeast Inner Mongolia and west Heilongjiang are irrigated, while the regions of southwest Henan and Qinling mountains, northeast and southwest of the Qinghai–Tibet Plateau, and the junction area of Shandong, Henan and Hebei are rain-fed. The regions of the southeast of the Qinghai–Tibet Plateau are fain-fed. Vegetation and precipitation in the southeast of the Qinghai–Tibet Plateau are significant negative correlation (R = −0.52), this is due to the adequate moisture conditions, vegetation growth is mainly limited to low temperatures. However, the occurrence of precipitation events leads to the increase of cloud cover and soil moisture, which further aggravates the harm of low temperature and indirectly inhibiting the growth of vegetation.

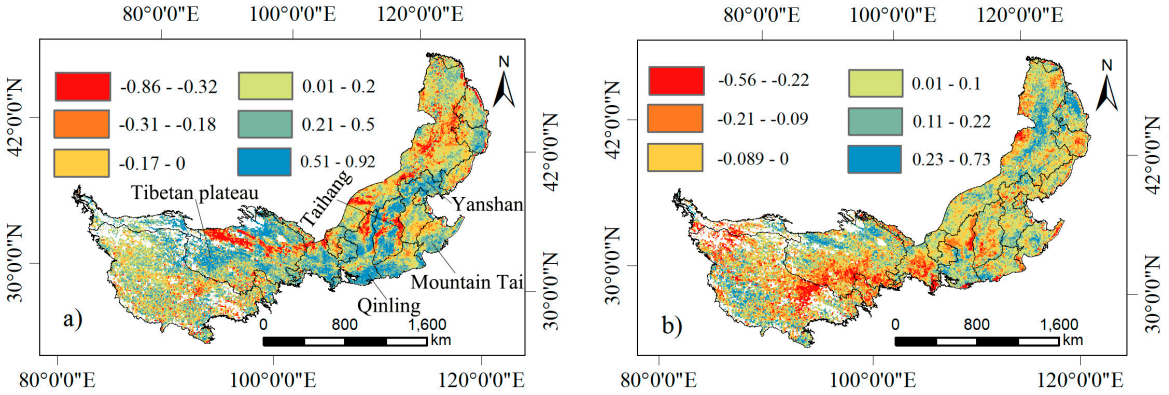

Figure 6. Partial correlation analysis between vegetation and temperature (**a**), precipitation (**b**) from 1982 to 2015.

3.2.2. Spatial Patterns of Vegetation under the Influence of Climate Change and Human Activities

Under the influence of climate change alone, the $NDVI_{pre}$ presented an obvious spatial differentiation from southeast to northwest, and the values gradually decreased from southeast to northwest (Figure 7a). Areas with good vegetation growth ($0.53 < NDVI_{pre} < 0.98$) accounted for 3.64% of the total area, mainly distributed in southern Shaanxi, eastern Gansu, and central Henan. The area with the lowest vegetation coverage ($-0.96 < NDVI_{pre} < 0.14$) was distributed in the northwest of Qinghai and Tibet, accounting for 29.52% of the total area. Figure 7b represents the spatial pattern of $NDVI_{res}$ under the influence of human activities alone; areas where human activities have a strong promoting effect on vegetation growth ($0.0025 < NDVI_{pre} < 0.008$) were mainly distributed in northern Shaanxi, eastern Gansu, Ningxia, southwestern Liaoning, Shandong, Henan, and Hebei, accounting for 5.95% of the total area. The regions where human activities inhibited vegetation growth ($-0.005 < NDVI_{pre} < 0$) were mainly distributed in the northeast of Inner Mongolia and the Greater Khingan mountains in the west of Heilongjiang, the Guanzhong Plain in the south of Shaanxi, central Henan Province, and the Taihang Mountains in the west of Hebei. In addition, the $NDVI_{res}$ values in Qinghai and central and western of Tibet were also negatively affected by human activities. These results lead us to infer that climatic changes have a higher impact on the NDVI in the study area than human activities, and the influence of human activities on vegetation growth is most pronounced in the central part of the study area.

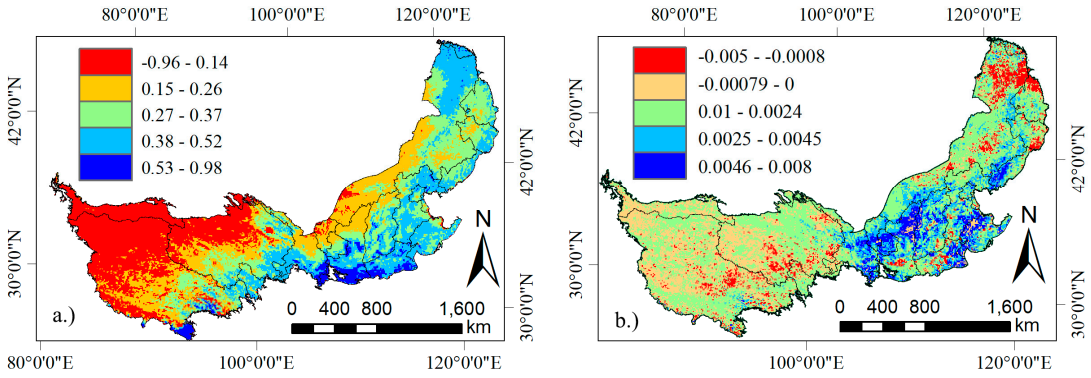

Figure 7. Spatial distribution of NDVI values under the impacts of climatic change (**a**) and human activities (**b**) from 1982–2015.

3.2.3. Vegetation Changes under the Influence of Climate Change and Human Activities

The interannual variation trend and significance test results of $NDVI_{pre}$ under the influence of climate change alone (Figure 8a,b) showed that 62.79% of the regions showed an increasing NDVI trend,

while 46.79% showed a significant increase ($P < 0.05$). The $NDVI_{pre}$ decreased in 37.21% of the regions and decreased significantly in 14.88% of the regions ($P < 0.05$). The regions with significantly increasing $NDVI_{pre}$ values were distributed in Shaanxi, Shanxi, northern Hebei, western Henan, and most of Qinghai, while the regions with significantly decreasing $NDVI_{pre}$ values were mainly distributed in the northwestern margin of Inner Mongolia. The regression analysis obtained the annual $NDVI_{pre}$ under the influence of climate change from 1982–2015. The $NDVI_{pre}$ significantly increased in Tibetan Plateau. The residual analysis method was used to obtain the annual vegetation $NDVI_{res}$ from 1982 to 2015 under the influence of human activities. The variation trend and significance test results of $NDVI_{res}$ under the influence of human activities alone showed that human activities positively impacted vegetation growth (Figure 8c,d); the $NDVI_{res}$ increased in 59.61% of the study area and increased significantly in 41.35% ($P < 0.05$). In contrast, 40.39% of the regions showed a decreasing $NDVI_{res}$ and 7.95% showed a significant decrease in $NDVI_{res}$ ($P < 0.05$). The regions where $NDVI_{res}$ increased significantly under the influence of human activities were concentrated in Shaanxi, Ningxia, Henan, Shanxi, Shandong, Hebei, the southeastern edges of Inner Mongolia and Qinghai, and northern Tibet. The $NDVI_{res}$ decreased significantly in the region between Inner Mongolia and Heilongjiang as well as in central Tibet and southwest of Qinghai.

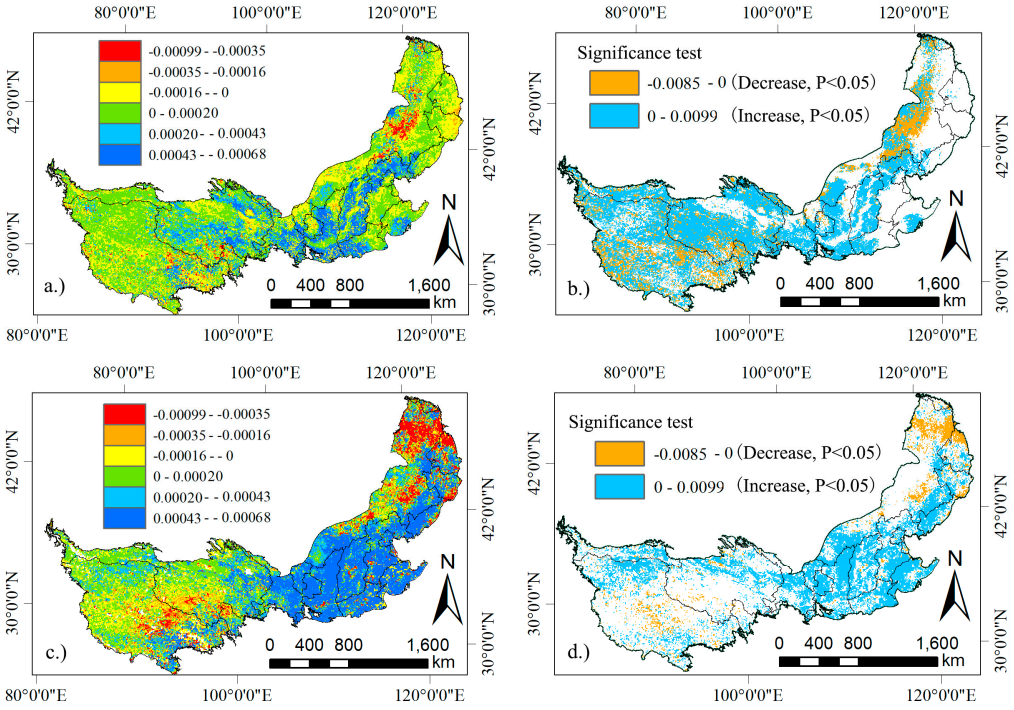

Figure 8. Sen's slope and Mann–Kendall (M–K) significance test of NDVI under the impacts of climate change (**a**,**b**) and human activities (**c**,**d**).

4. Discussion

From 1982 to 2015, the NDVI values in the fluctuation area of the 400 mm precipitation line showed an upward trend on both the seasonal scale and the annual scales, which was consistent with the NDVI variation trend obtained for different scales in global arid regions, Eurasia, China, and various river basins [47–49]. In 2019, *Nature* [50] and NASA [51] successively released research reports pointing out that China and India led the Earth to turn green, and the net increase in leaf area index in China accounted for 25% of the global total increase. This is also a partial confirmation of the gradual improvement of vegetation cover in China, which plays a role in reducing soil erosion and air pollution and in coping with the consequences of climatic changes. In this study, climatic factors (temperature and precipitation) played a positive role in promoting vegetation, while human

activities had an obviously positive and negative effect on the NDVI, which was similar to the results of previous studies [52]. Affected by the warm and humid airflow in the Indian Ocean, the vegetation condition in the southeast of the Qinghai–Tibet Plateau, with more suitable hydrothermal conditions, is significantly better than that in the northwest, which is consistent with the conclusions drawn from relevant studies [20,53]. The vegetation in the Greater Hinggan Mountains, in the northeast part of Inner Mongolia, shows a significant downward trend, mainly affected by factors such as decreased precipitation, increased evaporation caused by significant temperature increases, and more frequent droughts [54,55]. The vegetation on the Qinghai–Tibet Plateau showed a declining trend at both annual and seasonal scales, mainly because the continuous global warming results in higher spring temperatures in this region, which has relatively abundant water resources and is therefore suitable for grassland growth, however the grasslands are threatened by overgrazing [56].

The spatial distribution of the Hurst index values at different time scales indicates that in the southeast, with better hydrothermal conditions, the NDVI will significantly increase in the future. This is in line with the advanced agricultural technology, better agricultural irrigation facilities, adjustment of crop varieties and cropping systems, and mulching to adapt to climate change in the aforementioned areas. Although the NDVI will increase significantly, the regions with anti-persistence in the future will be concentrated in the northwest of Inner Mongolia and the north of Shaanxi, where the climatic conditions will be slightly less favorable. This region, located in the hinterland of the mainland, has the lowest precipitation, the largest evaporation, and an extreme water scarcity when compared with other regions at the same latitude. Droughts are further aggravated by the warmer and drier climate. Against with the background of long-term drying and warming, the vegetation is at risk of being permanently degraded, showing a poor adaptability to a changing climate. In general, in the future, the persistent of NDVI change tendency in the study area will be more negatively, which is consistent with the conclusion reached by Zhao et al. [57]. This shows that Hurst index method has good applicability in the analysis of vegetation change persistence characteristics in arid and semi-arid areas.

The change of temperature and precipitation has bidirectional regulating on vegetation growth. Before the temperature reaches the critical point where vegetation photosynthesis is most suitable, the increase of temperature will promote vegetation activities, but beyond the critical value of vegetation suitability, the consumption of nutrients by vegetation will be accelerated, and soil moisture evaporation will be intensified [58]. The temperature rise promoted the vegetation growth in the southeast of the study area and the Qinghai–Tibet Plateau with relatively good soil moisture, but inhibited the vegetation growth in the arid and rainless northwest. The increase of precipitation promoted the vegetation growth in most areas of Inner Mongolia with water-scarce, but inhibited the vegetation growth in the southeast of Qinghai–Tibet Plateau. Vegetation on both sides of the Yellow River at the junction of Shaanxi and Shanxi with relatively little annual precipitation should be positively correlated with precipitation, but the partial correlation analysis between precipitation and vegetation shows that vegetation is significantly negatively correlated with precipitation. The reason may be that the surface of this region is dominated by loess (one of loose soil type in semi-arid region of northwest China) which is easily eroded by precipitation. The soil erosion caused by precipitation offsets the benefits brought by precipitation for vegetation growth, making vegetation negatively correlated with precipitation. In the study of the relationship between vegetation growth and human activities, Deng et al. [59] proposed that human activities play a positive role in promoting vegetation growth in the Qinling Mountains. This paper found a similar phenomenon by quantitatively analyzing the impacts of human activities on vegetation, but the duality influence of human activities on vegetation in the study area was more typical. On the one hand, a series of ecological restoration projects (Grain for Green Program, Three-north Shelterbelt Forest Construction Project, Wildlife Protection and Nature Reserve Development Program) have generated a positively impact on the vegetation growth [60–64]. The national strategy of ecological civilization construction proposed by the Chinese government is to translate sustainable development into green development and build a beautiful

China, which is of great significance to improve a resident's environmental awareness [65]. In addition, agricultural irrigation facilities in arid and semi-arid areas have been continuously improved in recent years, the agricultural water-saving irrigation infrastructure has also been built to expand the area of water-saving irrigation [66]. On the other hand, in the process of industrialization, a large amount of land is being changed into construction land, resulting in the increase of impermeable water surface and decrease of vegetation coverage. The unreasonable exploitation of natural resources implemented by resource-based cities and the rapid expansion of large and medium-sized cities have resulted in the serious degradation of vegetation, especially for some cities in Henan, Shaanxi, Shanxi, and Inner Mongolia [67].

The change of one element in a geographical system inevitably affects the change of other elements. Therefore, a partial correlation analysis method was adopted in this study to examine the correlation between vegetation and temperature, precipitation by controlling relevant variables, so that the analysis results can more accurately depict the correlation between vegetation and climate factors. The interactions among vegetation, climate change, and human activities are highly complex, and the stability of different vegetation types and their adaptability to climate change vary greatly. In this sense, further studies will have to analyze the impacts of climate change on different vegetation types. In this study, we only used temperature and precipitation, which have the most obvious influence on vegetation growth, when analyzing the influence of climate on vegetation changes. However, any changes in vegetation are the result of the comprehensive action of various elements (temperature, precipitation, soil, solar radiation, topography and human activities), and these elements should be considered more comprehensively to objectively quantify the internal driving mechanisms of vegetation change. Therefore, in the following study, the authors will collect all kinds of climatic factors affecting vegetation growth and screen them based on the stepwise regression method in order to obtain the main climatic factors affecting vegetation growth. On this basis, the geographical weighted regression method may be used to analyze the impact of climate factors on dynamic changes of vegetation, and the human variation coefficient model may be constructed to evaluate the impact of human activities on vegetation changes. In addition, in the partial correlation analysis between climate factors and vegetation, the two variables of temperature and humidity, which have the most significant influence on vegetation, were taken into account. However, evapotranspiration has a direct impact on water conditions, which may increase the uncertainty of the analysis results. Therefore, the second-order partial correlation analysis method is required in the following study to take temperature, precipitation and evapotranspiration into account regarding the impact factor of vegetation. The multiple regression analysis method was used to separate the effects of climate change and human activities on vegetation, and the comparative study found that this study achieved relatively ideal and accurate results. This verifies the adaptability of this method in this field, which is similar to the conclusion reached by relevant scholars [68,69].

5. Conclusions

The interannual changes of vegetation in the fluctuation area of the 400 mm precipitation line show a spatio-temporal heterogeneity, with a growth rate of 0.50%/10a. On the seasonal scale, the increase rate of NDVI in autumn was the highest (0.79%/10a), followed by those for spring and summer. Spatially, vegetation growth in the southeast and central regions of the study area showed a significant upward trend ($P < 0.05$), while the vegetation in the northeast (−2.3%/10a) and southwest (−1.4%/10a) regions decreased significantly. Along with the seasonal changes, the area with significant NDVI changes retreated from southeast to northwest.

Under the influence of climatic factors alone, the spatial pattern of $NDVI_{pre}$ showed a spatial differentiation from southeast to northwest, and the values gradually decreased from southeast to northwest. The areas where human activities had a positive impact on vegetation, with a relatively high impact, accounted for 5.95% of the total area of the study area. Areas where the vegetation cover was reduced as a result of human activities were mainly distributed in the northeast of Inner Mongolia

and the Greater Hinggan Mountains in the west of Heilongjiang, the Guanzhong Plain in the south of Shaanxi, the Taihang Mountains in the central of Henan and the west of Hebei, and the central and western parts of Qinghai and Tibet. Under the influence of climate change alone, the area of $NDVI_{pre}$ that increased accounted for 62.79% of the total area, of which 46.79% increased significantly ($P < 0.05$). The area with decreasing $NDVI_{pre}$ values accounted for 37.21% of the total area, and the decreasing area of 14.88% was significant ($P < 0.05$). Under the influence of human activities, the vegetation $NDVI_{res}$ in the study area from 1982 to 2015 was mainly increased on an annual scale, and the area that passed the significance test ($P < 0.05$) accounted for 41.35% of the total area, and the area that showed a decreasing trend and passed the significance test only accounted for 7.95% of the total area.

In this study, the authors using the dataset of GIMMS NDVI3g with the spatial resolution of 8 × 8 km, data fusion technology could be adopted to combine MODIS NDVI with the spatial resolution of 250 × 250 m or other image data with higher resolution to improve the spatial resolution of GIMMS NDVI3g (1982–2000) in the future. Furthermore, by combining high-resolution remote sensing image data (MODIS NDVI) from 2001 to 2015, high-resolution image datasets of the past 34 years were obtained, which is beneficial to study the response of vegetation dynamics to climate change and human activities in a more detailed way. In addition, the impacts of human activities and climate change on vegetation dynamics were separated, and the impacts of climate change and human activities on vegetation were quantitatively analyzed in this study. However, the impacts of climate factors of various types (temperature, precipitation, relative humidity, solar radiation, soil moisture and evaporation) and types of human activities (ecological restoration projects, agricultural technical measures and urban construction) on vegetation were not specifically quantified. Therefore, how to build a model for quantifying the various influence factors of on vegetation at a more precise scale is a challenge that needs to be solved.

Author Contributions: Conceptualization, Y.L. and Y.Q.; Data curation, Z.X. and Z.Z.; Formal analysis, Z.Z.; Methodology, Y.L.; Writing – original draft, Y.L.; Writing – review and editing, Z.X. and Y.Q.

Funding: This research was supported and funded by the National Natural Science Foundation of China (No.41671536; No.41501588), and the International Cooperation Laboratory of Geospatial Technology for Henan province (No.152102410024).

Acknowledgments: The authors would like to pay special thanks to the National Science and Technology Infrastructure of China, Data Sharing Infrastructure of Earth System Science -Data Center of Lower Yellow River Regions (http://henu.geodata.cn).

Conflicts of Interest: The authors declared no conflict of interest.

References

1. IPCC. *Climate Change 2013: The Physical Science Basis. Contribution of Working Group I to the Fifth Assessment Report of the Intergovernmental Panel on Climate Change*; Stocker, T.F., Qin, D., Plattner, G.-K., Tignor, M., Allen, S.K., Boschung, J., Nauels, A., Xia, Y., Bex, V., Midgley, P.M., Eds.; Cambridge University Press: Cambridge, UK, 2013; 1535p.
2. Buitenwerf, R.; Rose, L.; Higgins, S.I. Three decades of multi-dimensional change in global leaf phenology. *Nat. Clim. Chang.* **2015**, *5*, 364–368. [CrossRef]
3. Verbeeck, H.; Kearsley, E. The importance of including lianas in global vegetation models. *Proc. Natl. Acad. Sci. USA* **2016**, *113*, E4. [CrossRef] [PubMed]
4. Fensholt, R.; Rasmussen, K.; Nielsen, T.T.; Mbow, C. Evaluation of earth observation based long term vegetation trends—Intercomparing NDVI time series trend analysis consistency of Sahel from AVHRR GIMMS, TERRA MODIS and SPOT VGT data. *Remote Sens. Environ.* **2009**, *113*, 1886–1898. [CrossRef]
5. Rasmus, F.; Simon, R.P. Evaluation of Earth Observation based global long term vegetation trends—Comparing GIMMS and MODIS global NDVI time series. *Remote Sens. Environ.* **2012**, *119*, 131–147.
6. Tucker, C.J. Red and photographic infrared linear combinations for monitoring vegetation. *Remote Sens. Environ* **1979**, *8*, 127–150. [CrossRef]

7. Forkel, M.; Carvalhais, N.; Verbesselt, J.; Mahecha, M.; Neigh, C.; Reichstein, M. Trend change detection in NDVI time series: Effects of inter-annual variability and methodology. *Remote Sens.* **2013**, *5*, 2113–2144. [CrossRef]
8. Mueller, T.; Dressler, G.; Tucker, C.J.; Pinzon, J.E.; Leimgruber, P.; Dubayah, R.O.; Hurtt, G.C.; Bohning-Gaese, K.; Fagan, W.F. Human land-use practices lead to global long-term increases in photosynthetic capacity. *Remote Sens.* **2014**, *6*, 5717–5731. [CrossRef]
9. Ma, Z.H.; Peng, C.H.; Zhu, Q.; Chen, H.; Yu, G.R.; Li, W.Z.; Zhou, X.L.; Wang, W.F.; Zhang, W.H. Regional drought-reduced reduction in the biomass carbon sink of Canada's boreal forests. *Proc. Natl. Acad. Sci. USA* **2012**, *109*, 2423–2427. [CrossRef]
10. Eastman, J.R.; Sangermano, F.; Machado, E.A.; Rogan, J.; Anyamba, A. Global trends in seasonality of normalized difference vegetation index (NDVI), 1982–2011. *Remote Sens.* **2013**, *5*, 4799–4818. [CrossRef]
11. Jiang, N.; Zhu, W.; Zheng, Z.; Chen, G.; Fan, D.A. Comparative Analysis between GIMSS NDVIg and NDVI3g for Monitoring Vegetation Activity Change in the Northern Hemisphere during 1982–2008. *Remote Sens.* **2013**, *5*, 4031–4044. [CrossRef]
12. Zhou, Z.Y.; Sun, O.J.; Huang, J.H.; Li, L.H.; Liu, P.; Han, X.G. Soil carbon and nitrogen stores and storage potential as affected by land use in an Agro-pastoral ecotone of northern China. *Biogeochemistry* **2007**, *82*, 127–138. [CrossRef]
13. Zhao, H.L.; Zhao, X.Y.; Zhang, T.H.; Zhou, R.L. Boundary line on Agro-pasture zigzag zone in north China and its problems on eco-environment. *Adv. Earth Sci.* **2002**, *17*, 739–747.
14. Zhao, Z.W.; Zhang, L.; Li, X.; Wang, Y.X.; Wang, S.L. Monitoring vegetation dynamics during the growing season in Ningxia based on MOD13Q1 data. *Prog. Geogr.* **2017**, *36*, 741–752.
15. Zhang, C.; Lei, T.W.; Song, T.X. Analysis of temporal and spatial characteristics of time lag correlation between the vegetation cover and soil moisture in the Loess Plateau. *Acta Ecol. Sin.* **2018**, *38*, 2128–2138.
16. Gao, H.D.; Pang, G.W.; Zhang, Z.B.; Cheng, S.D. Evaluating the potential of vegetation restoration in the Loess Plateau. *Acta Geogr. Sin.* **2017**, *72*, 863–874.
17. Liu, D.; Yu, C.L. Effects of climate change on the distribution of main vegetation types in Northeast China. *Acta Geogr. Sin.* **2017**, *37*, 6511–6522.
18. Wang, Z.M.; Luo, L.; Song, K.S.; Liu, D.W.; Zhang, B.; Song, C.C. Growing-season normal difference vegetation index, NDVI, response to climate changes and increased carbon dioxide concentration in frozen areas of Northeast China during 1982–2008. *Acta Sci. Circumstantiae* **2010**, *30*, 2332–2343.
19. Wang, X.; Jin, R.; Du, P.J.; Liang, H. Trend of surface freeze-thaw cycles and vegetation green-up date and their response to climate change on the Qinghai-Tibet Plateau. *J. Remote Sens.* **2018**, *22*, 508–520.
20. Zhuo, G.; Chen, S.R.; Zhou, Y.B. Spatio-temporal variation of vegetation coverage over the Tibetan Plateau and its responses to climatic factors. *Acta Ecol. Sin.* **2018**, *38*, 3208–3218.
21. Zhang, G.L.; Ouyang, H.; Zhang, X.Z.; Zhang, C.P.; Xu, X.L. Vegetation change and its responses to climatic variation based on eco-geographical regions of Tibetan Plateau. *Geogr. Res.* **2010**, *8*, 88–95.
22. Shi, X.L.; Shi, W.J. Review on boundary shift of farming-pastoral ecotone in northern China and its driving forces. *Trans. Chin. Soc. Agric. Eng.* **2018**, *34*, 1–11.
23. Shi, X.; Wang, W.; Shi, W. Progress on quantitative assessment of the impacts of climate change and human activities on cropland change. *J. Geogr. Sci.* **2016**, *26*, 339–354. [CrossRef]
24. Ye, Y.; Fang, X.Q.; Ren, Y.Y.; Zhang, X.Z.; Chen, L. Cropland cover change in northeast China during the past 300 years. *Sci. China Ser. D Earth Sci.* **2009**, *52*, 1172–1182. [CrossRef]
25. Sun, W.Y.; Song, X.Y.; Mu, X.M.; Gao, P.; Wang, F.; Zhao, G.J. Spatiotemporal vegetation cover variations associated with climate change and ecological restoration in the Loess Plateau. *Agric. For. Meteorol.* **2015**, *209*, 87–99. [CrossRef]
26. Feng, X.M.; Fu, B.J.; Piao, S.L.; Wang, S.; Ciais, P.; Zeng, Z.Z.; Lü, Y.H.; Zeng, Y.; Li, Y.; Jiang, X.H.; et al. Revegetation in China's Loess Plateau is approaching sustainable water resource limits. *Nat. Clim. Chang.* **2016**, *6*, 1019–1022. [CrossRef]
27. Fang, J.Y.; Piao, S.L.; He, J.S.; Ma, W.H. Increasing terrestrial vegetation activity in China, 1982–1999. *Sci. China (Ser. C Life Sci.)* **2004**, *47*, 229–240.
28. Bao, G.; Bao, Y.H.; Yang, Z.H.; Zhou, Y.; Shiirew, A. Vegetation Cover Changes in Mongolian Plateau and Its Response to Seasonal Climate Changes in Recent 10 Years. *Sci. Geogr. Sin.* **2013**, *33*, 613–621.

29. Zhao, X.; Hu, H.; Shen, H.; Zhou, D.; Zhou, L.; Myneni, R.B.; Fang, J. Satellite-indicated long-term vegetation changes and their drivers on the Mongolian Plateau. *Landsc. Ecol.* **2015**, *30*, 1599–1611. [CrossRef]
30. Cai, B.F.; Yu, R. Advance and evaluation in the long time series vegetation trends research based on remote sensing. *J. Remote Sens.* **2009**, *13*, 1170–1186.
31. Liu, Y.; Li, Y.; Li, S.C.; Motesharrei, S. Spatial and Temporal Patterns of Global NDVI Trends: Correlations with Climate and Human Factors. *Remote Sens.* **2015**, *7*, 13233–13250. [CrossRef]
32. Li, S.J.; Li, X.B.; Tan, M.H. Impacts of rural-urban migration on vegetation cover in eco-logically fragile areas: Taking Inner Mongolia as a case. *Acta Geogr. Sin.* **2015**, *70*, 1622–1631.
33. Li, X.M.; Ren, Z.Y.; Zhang, C. Spatial-temporal variations of vegetation cover in Chongqing city (1999–2010): Impacts of climate factors and human activities. *Sci. Geogr. Sin.* **2013**, *33*, 1390–1394.
34. Li, Y.; Qin, Y.C. The Response of Net Primary Production to Climate Change: A Case Study in the 400 mm Annual Precipitation Fluctuation Zone in China. *Int. J. Environ. Res. Public Health* **2019**, *16*, 1497. [CrossRef]
35. Zhou, D.; Zhao, S.; Zhu, C. The Grain for Green Project induced land cover change in the Loess Plateau: A case study with Ansai County, Shanxi Province, China. *Ecol. Indic.* **2012**, *23*, 88–94. [CrossRef]
36. Evans, J.; Geerken, R. Discrimination between climate and human-induced dryland degradation. *J. Arid Environ.* **2004**, *57*, 535–554. [CrossRef]
37. Geerken, R.; Ilaiwi, M. Assessment of rangeland degradation and development of a strategy for rehabilitation. *Remote Sens. Environ.* **2004**, *90*, 490–504. [CrossRef]
38. Gitelson, A.A.; Kaufman, Y.J.; Stark, R.; Rundquist, D. Novel algorithms for remote estimation of vegetation fraction. *Remote Sens. Environ.* **2002**, *80*, 76–87. [CrossRef]
39. Liu, X.F.; Pan, Y.Z.; Zhu, X.F.; Li, S.S. Spatiotemporal variation of vegetation coverage in Qinling-Daba Mountains in relation to environmental factors. *Acta Geogr. Sin.* **2015**, *70*, 705–716.
40. Liu, B.; Sun, Y.L.; Wang, Z.L.; Zhao, T.B. Analysis of the vegetation cover change and the relative role of its influencing factors in North China. *J. Nat. Resour.* **2015**, *30*, 12–23.
41. Li, J.; Peng, S.; Li, Z. Detecting and attributing vegetation changes on China's Loess Plateau. *Agric. For. Meteorol.* **2017**, *247*, 260–270. [CrossRef]
42. Hurst, E.H. Long-term storage capacity of reservoirs. *Trans. Am. Soc. Civ. Eng.* **1951**, *116*, 770–808.
43. Ray, R.; Khondekar, M.H.; Ghosh, K.; Bhattacharjee, A.K. Scaling and nonlinear behaviour of daily mean temperature time series across India. *Chaos Solitons Fractals* **2016**, *84*, 9–14. [CrossRef]
44. Rehman, S. Study of Saudi Arabian climatic conditions using Hurst exponent and climatic predictability index. *Chaos Solitons Fractals* **2009**, *39*, 499–509. [CrossRef]
45. Fang, L.; Wang, W.J.; Jiang, W.G.; Chen, M.; Wang, Y.; Jia, K.; Li, Y.S. Spatio-temporal Variations of Vegetation Cover and Its Responses to Climate Change in the Heilongjiang Basin of China from 2000 to 2014. *Sci. Geogr. Sin.* **2017**, *37*, 1745–1754.
46. Deng, Z.Y.; Wang, Q.; Zhang, Q.; Qing, J.Z.; Yang, Q.G.; Yuan, Z.P.; Liu, W.J.; Xu, J.F. Impact of climate warming and drying on food crops in northern China and the countermeasures. *Acta Ecol. Sin.* **2010**, *30*, 6278–6288.
47. Chen, C.N.; Zhu, L.Q.; Tian, L.; Li, X.G. Spatial-temporal changes in vegetation characteristics and climate in the Qinling-Daba Mountains. *Acta Ecol. Sin.* **2019**, *39*, 1–9.
48. Yuan, L.H.; Jiang, W.G.; Shen, W.M.; Liu, Y.H.; Wang, W.J.; Tao, L.L.; Zheng, H.; Liu, X.F. The Spatio-temporal variations of vegetation cover in the Yellow River Basin from 2000 to 2010. *Acta Ecol. Sin.* **2013**, *33*, 7798–7806.
49. Fan, N.; Xie, G.D.; Zhang, C.S.; Chen, L.; Li, W.H.; Cheng, S.K. Spatial-temporal dynamic changes of vegetation cover in Lancang river basin during 2001–2010. *Resour. Sci.* **2012**, *34*, 1222–1231.
50. Chen, C.; Park, T.; Wang, X.H.; Piao, S.L.; Xu, B.D.; Rajiv, K.C.; Richard, F.; Victor, B.; Philippe, C.; Fensholt, R.; et al. China and India lead in greening of the world through land-use management. *Nat. Sustain.* **2019**, *2*, 122–129. [CrossRef]
51. NASA. Human Activity in China and India Dominates the Greening of Earth, NASA Study Shows. Available online: https://www.nasa.gov/feature/ames/human-activity-in-china-and-india-dominates-the-greening-of-earth-nasa-study-shows (accessed on 12 February 2019).
52. Luan, J.k.; Liu, D.F.; Huang, Q.; Feng, J.L.; Li, G.B. Analysis of the spatial-temporal change and impact factors of the vegetation index in Yulin, Shaanxi Province, in the last 17 years. *Acta Ecol. Sin.* **2018**, *38*, 2780–2790.
53. Li, J.C.; Wang, J.R.; Gong, B.; Gan, X.L.; Hu, W.W.; Liu, W.L. Spatiotemporal changes of vegetation cover in response to climate change on the Tibetan Plateau. *Acta Geol. Sin.* **2014**, *88*, 974–983. [CrossRef]

54. Ma, Z.G.; Ren, X.B. Drying Trend over China from 1951 to 2006. *Adv. Clim. Chang. Res.* **2007**, *3*, 195–201.
55. Sun, Y.G.; Bai, R.H.; Xie, A. Interdecadal Variations of Droughts in Northeastern China. *Acta Scicentiarum Nat. Univ. Pekinesis* **2004**, *40*, 806–813.
56. Xu, Y.L.; Zheng, D.W.; Liu, X.Y.; Zhao, Y.X.; Ma, C.S.; Li, K. *Studies on Critical Issues of Agriculture Adaptation to Climate Change in China*; China Meteorological Press: Beijing, China, 2014.
57. Zhao, A.Z.; Zhang, A.B.; Liu, H.X.; Liu, Y.X.; Wang, H.F.; Wang, D.L. Spatiotemporal Variation of Vegetation Coverage before and after Implementation of Grain for Green Project in the Loess Plateau. *J. Nat. Res.* **2017**, *32*, 449–460.
58. Zhang, K.; Kimball, J.S.; Nemani, R.R.; Running, S.W.; Hong, Y.; Gourley, J.J.; Yu, Z.B. Vegetation greening and climate change promote multidecadal rises of global land evapotranspiration. *Sci. Rep.* **2015**, *5*, 15956. [CrossRef]
59. Deng, C.H.; Bai, H.Y.; Gao, S.; Liu, R.J.; Ma, X.P.; Huang, X.Y.; Meng, Q. Spatial-temporal variation of the vegetation coverage in Qinling mountains and its dual response to climate change and human activities. *J. Nat. Res.* **2018**, *33*, 425–438.
60. Yan, E.P.; Lin, H.; Dang, Y.F.; Xia, C.Z. The spatiotemporal changes of vegetation cover in Beijing-Tianjin sandstorm source control region during 2000–2012. *Acta Ecol. Sin.* **2014**, *34*, 5007–5020.
61. Liu, X.; Zhu, X.; Pan, Y.; Li, S.; Ma, Y.; Nie, J. Vegetation dynamics in Qinling-Daba mountains in relation to climate factors between 2000 and 2014. *J. Geogr. Sci.* **2016**, *26*, 45–58. [CrossRef]
62. Zhang, L.; Ding, M.J.; Zhang, H.M.; Wen, C. Spatiotemporal variation of the vegetation coverage in Yangtze river basin during 1982–2015. *J. Nat. Res.* **2018**, *33*, 2084–2097.
63. Zhang, P.; Shao, G.; Zhao, G.; Le Master, D.C.; George, R.P.; John, B.D.; Li, Q. China's forest policy for the 21st century. *Science* **2000**, *288*, 2135–2136. [CrossRef]
64. Li, Y.; Xie, Z.; Qin, Y.; Sun, Y. Temporal-Spatial Variation Characteristics of Soil Erosion in the Pisha Sandstone Area, Loess Plateau, China. *Pol. J. Environ. Stud.* **2019**, *28*, 2205–2214. [CrossRef]
65. The State Council of the People's Republic of China. The 13th Five-Year Plan for Ecological and Environmental Protection. Available online: http://www.gov.cn/zhengce/content/2016-12/05/content_5143290.htm (accessed on 5 December 2016).
66. Xing, H.N.; Yang, Q.L.; Yu, L.M.; Liu, X.G. Design and experiment of sprinkler irrigation device with square spray field. *Trans. Chin. Soc. Agric. Eng.* **2017**, *33*, 84–91.
67. Liu, Y.X.; Liang, X.; Liu, X.F. Study on the Spatial Optimizing and Coordination of Cities and Ground Vegetation Under the Background of Ecological Restoration in Guanzhong Region. *J. Nat. Res.* **2013**, *28*, 1515–1525.
68. Zheng, K.; Wei, J.Z.; Pei, J.Y.; Zhang, X.L.; Huang, F.Q.; Li, F.M.; Ye, J.S. Impacts of climate change and human activities on grassland vegetation variation in the Chinese Loess Plateau. *Sci. Total Environ.* **2019**, *660*, 236–244. [CrossRef]
69. Wang, J.; Wang, K.; Zhang, M.; Zhang, C. Impacts of climate change and human activities on vegetation cover in hilly southern China. *Ecol. Eng.* **2015**, *81*, 451–461. [CrossRef]